Mechanical Properties of CAC Under Biaxial Compression: A 3D Mesoscopic Study

CHEN Xusheng¹, MA Haiyan^{1,2*}, YU Hongfa^{1*}

1. College of Civil Aviation, Nanjing University of Aeronautics and Astronautics, Nanjing 211106, P. R. China; 2. College of Intelligent Construction, Jishou University, Zhangjiajie 427000, P. R. China

(Received 23 May 2025; revised 16 July 2025; accepted 4 August 2025)

Abstract: Studies on coral aggregate concrete (CAC) mainly focus on uniaxial stress conditions. However, concrete structures often experience complex stress conditions in practical engineering. It is essential to investigate the mechanical behavior and failure mechanisms of CAC under multiaxial stress conditions. This paper employs a 3D mesoscale model that considers the actual size, shape, and spatial distribution of aggregates. The reliability of the model and material parameters is verified through comparison with existing experimental data. Subsequently, the model is used to systematically study the mechanical properties, failure modes, and failure processes of C40 CAC under the biaxial compression. The numerical results are compared with the experimental results of CAC and ordinary portland concrete (OPC). The results indicate that the failure modes of CAC under the biaxial compression are diagonal shear failure. The biaxial compressive strength and elastic modulus of CAC are greater than those under uniaxial stress and exhibit a significant intermediate principal stress effect. The biaxial compressive strength reaches its maximum value when the stress ratio is 0.5, which is consistent with the conclusions for OPC. Finally, failure criteria and strength envelopes for CAC under the biaxial compression are established in order to provide a reference for analyzing the strength characteristics and structural design of CAC.

Key words: coral aggregate concrete (CAC); biaxial compression; stress ratio; failure mode; strength envelope **CLC number:** TU528 **Document code:** A **Article ID:** 1005-1120(2025)S-0156-11

0 Introduction

In recent decades, engineering construction projects on islands in the South China Sea have been continuously advanced. However, these islands are situated a considerable distance from the mainland, facing harsh environmental conditions and lacking in sand, gravel, and freshwater resources. Coral aggregate concrete (CAC) is prepared using coral debris and coral sand as coarse and fine aggregates, mixed with seawater. It is used in island construction projects such as harbors, breakwaters, and roadways. This approach reduces the high cost associated with transporting building materials over long distances and effectively shortens construction periods, all while preserving reef environments and

natural ecosystems. It holds significant engineering practical value^[1].

Coral aggregates are characterized by high porosity, low strength, and high brittleness^[2], which make the mechanical properties of CAC different from those of ordinary portland concrete (OPC). Theories related to OPC cannot be directly applied to CAC. Therefore, theoretical and experimental studies specific to CAC are particularly important. Da et al.^[3], Mi et al.^[4], and Su et al.^[5] investigated the basic mechanical properties and uniaxial compressive mechanical properties of CAC. They obtained uniaxial compressive stress-strain curves of CAC and established corresponding constitutive models. The above research primarily focuses on uniaxial stress conditions and derives conclusions

How to cite this article: CHEN Xusheng, MA Haiyan, YU Hongfa. Mechanical properties of CAC under biaxial compression: A 3D mesoscopic study[J]. Transactions of Nanjing University of Aeronautics and Astronautics, 2025, 42(S): 156-166. http://dx.doi.org/10.16356/j.1005-1120.2025.S.014

^{*}Corresponding authors, E-mail addresses: mahaiyan@nuaa.edu.cn; yuhongfa@nuaa.edu.cn.

based on linear elasticity theory. However, in actual engineering structures, concrete is often subjected to complex stress states, such as in breakwaters, roads, and joints of frame structures. Concrete is a complex and variable material, with various strengths, mechanical properties, and deformations differing from those under uniaxial stress conditions. Therefore, to meet the demands of practical engineering and enrich the theoretical foundation, it is necessary to study the mechanical behavior of concrete under complex stress states.

In recent years, domestic scholars have gradually begun to study the multiaxial mechanical properties of CAC. Li^[6] conducted experimental research on the biaxial compressive behavior of CAC and found that its biaxial compressive strength was related to the stress ratio. When the stress ratio is 0.5, the biaxial compressive strength of CAC reaches its maximum value. Wu et al.^[7] performed numerical simulations of the biaxial mechanical properties of C30 CAC under different conditions and analyzed its failure process and failure mechanism.

This study employs a 3D mesoscale model that considers the shape, size, and distribution of coral aggregates to simulate the biaxial compressive mechanical behavior of C40 CAC under different stress ratios. The HJC model^[8] and the K&C model^[9] are used to describe the material behavior of coral aggregates and mortar, respectively. The material parameters for CAC are determined based on existing experimental results. Furthermore, the numerical results are validated against existing uniaxial and biaxial compression test results for CAC^[6] to confirm the reliability and accuracy of the model. Subsequently, the validated mesoscale model is used to simulate the biaxial mechanical properties of CAC and obtain the failure modes and stress-strain curves under different conditions. Finally, the corresponding failure envelopes and strength criteria are established. This research holds significant scientific and engineering value for the analysis of CAC's mechanical behavior and structural design, providing theoretical support for the application of CAC in practical engineering projects.

1 3D Mesoscale Model and Material Model Under Biaxial Loads

1. 1 3D mesoscale geometry model

To investigate the biaxial compressive mechanical properties of CAC, this study employs the mesoscale modeling approach proposed by Wu et al. [7] to construct a cubic concrete model with a side length of 100 mm, as depicted in Fig.1, where ITZ denotes the interfacial transition zone. The aggregate model in this paper is a 3D random model that considers the randomness in shape, size, and spatial distribution of aggregates, as illustrated in Fig.2. Based on the generated 3D random aggregate model, a 3D concrete mesoscale model is established using a spatial random placement algorithm. This model takes into account coarse aggregates, mortar, and ITZ. Subsequently, the model is spatially partitioned using spatial mapping grid partitioning algorithms and material identification algorithms. This results in the corresponding 3D finite element mesoscale model which will be used for subsequent numerical calculations and analysis of CAC^[7].

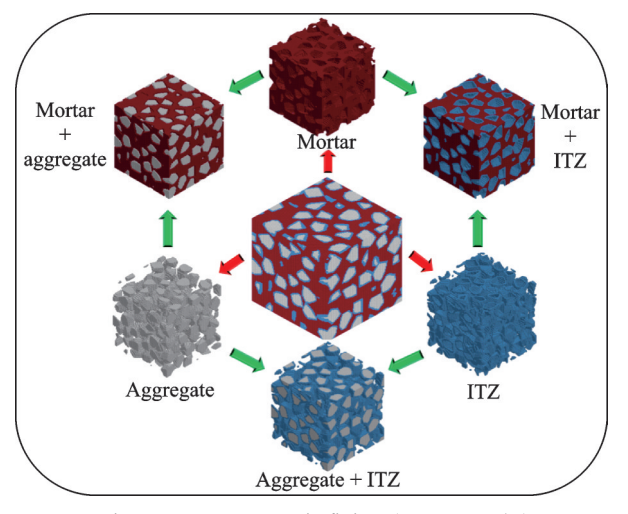
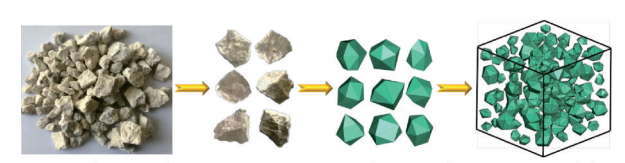


Fig.1 3D mesoscopic finite element model



Broken coral aggregates 3D random coral aggregate model

Fig.2 3D random aggregate model

Concrete is considered to be composed of aggregates, mortar, and ITZ at the mesoscale. In Fig.1, different colors are used to represent different mesoscopic components: Mortar (red), ITZ (blue), and coral aggregates (white). The mesh size used in this study is 1 mm, with a total of 1 000 000 elements. Specifically, there are 521 531 mortar units, 272 155 aggregate units, and 206 314 ITZ units.

In the mesoscale model presented in this study, the ITZ thickness is set greater than that of actual thickness in concrete. Previous studies have shown that the ITZ is a thin layer between the aggregate and mortar, with a typical thickness of approximately 10 — 50 µm^[10]. However, in finite element analysis of concrete, meshing the ITZ with elements at the micron scale is impractical, as it is both time-consuming and inefficient for numerical computation. Moreover, setting the ITZ thickness too small makes it difficult to accurately capture the initiation and propagation of cracks within the ITZ, as well as the overall fracture behavior. Considering both computational accuracy and efficiency, the minimum element size in this study is set to 1 mm, and the ITZ thickness is defined as 1-2 mm.

1. 2 Concrete material model and parameters

Based on the physical and mechanical characteristics of each mesoscopic component, the *MAT_CONCRETE_DAMAGE_REL3 (K&C) material model (MAT_072R3) and the *MAT_JOHNSON_HOLMQUIST_CONCRETE (HJC) material model (MAT_111) in LS-DYNA are chosen to simulate the mechanical behavior of ITZ for mortar and coral aggregates, respectively. This study focuses on C40 CAC and the calculation parameters for the material models can be found in Table 1.

Table 1 Material parameters of CAC

Material	Mass density ρ / (kg•m ⁻³)	Uniaxial compressive strength $f_{\rm c}/$	Uniaxial tensile strength f_t /	Poisson's ratio μ
		MPa	MPa	
Mortar	2 350	43	4.8	0.21
ITZ	1 880	21	3.1	0.21
Aggregate	2 550	10	1.4	0.16

1. 2. 1 K&C model

Three independent shear failure surfaces (Eq.(1)) are used to characterize the material behavior of concrete. The strain rate effect can be reflected in the failure surface using the dynamic increase factor (DIF), as shown in Eq.(2). The EOS_TABULATED_COMPACTION (EOS_8) in LS-DYNA is used to define the relationship between the pressure and volume strain, as shown in Eq.(3). Moreover, the fracture energy $G_{\rm f}$ can be calculated by means of the area under the stress-strain curve to make sure that the results will be objective on mesh refinement, which is expressed as Eq.(4).

$$\begin{cases} \Delta \sigma_{y} = a_{0y} + p/(a_{1y} + a_{2y}p) \\ \Delta \sigma_{m} = a_{0} + p/(a_{1} + a_{2}p) \\ \Delta \sigma_{r} = p/(a_{1f} + a_{2f}p) \end{cases}$$
(1)

$$\Delta \lambda = b_3 f_{\rm d} k_{\rm d} (\varepsilon_{\rm V} - \varepsilon_{\rm V, vield}) \tag{2}$$

$$P = C(\varepsilon_{V}) + \gamma_{0} T(\varepsilon_{V}) E \tag{3}$$

$$G_{\rm f} = h_{\rm c} \int \sigma \mathrm{d}\varepsilon$$
 (4)

where $\Delta \sigma_{\rm y}$, $\Delta \sigma_{\rm m}$ and $\Delta \sigma_{\rm r}$ represent the yield failure surface, the maximum failure surface and the residual failure surface, respectively; a_i , a_{iy} , and a_{it} (where i=0, 1, and 2) the material constants associated with the compressive and tensile strength of concrete; and γ_0 and T the temperature parameters. $k_{\rm d}$ represents an internal scalar multiplier; b_3 the damage scaling coefficient for triaxial tension; $f_{\rm d}$ the scalar used to restrict the effect of the volumetric damage; p the pressure; $C(\varepsilon_{\rm V})$ the pressure-volume function; E the initial internal energy; σ the actual equivalent stress; and $h_{\rm c}$ the characteristic length of element.

1.2.2 HJC model

The HJC model is commonly used to describe the material behavior of concrete materials under various loading conditions. This model considers the influence of pressure, strain rate, material damage, and other factors on the equivalent strength of concrete. The normalized equivalent stress can be expressed as

$$\sigma^* = \sigma/f_{\rm c}' \tag{5}$$

$$\sigma^* = [A(1-D) + B(p^*)^N][1 - C \ln \dot{\varepsilon}^*]$$
 (6)

where σ^* represents the normalized equivalent stress; $f_{\rm c}'$ the quasi-static uniaxial compressive strength; A the normalized cohesive strength; B the normalized pressure hardening; C the strain rate coefficient; D the damage parameter; $\dot{\epsilon}^*$ the normalized equivalent strain; and $p^* = p/f_{\rm c}'$ the normalized pressure.

In the HJC model, the strain rate coefficient C governs the slope of the increase in strength with respect to the logarithm of the strain rate, $\ln \dot{\epsilon}^*$, effectively controlling the rate of dynamic strength enhancement. A larger C value indicates higher strainrate sensitivity of the material, meaning that the dynamic strength increases more significantly relative to the quasi-static strength under the same strain rate. The strain rate coefficient directly influences the predicted dynamic strength in the model. If C is set too high, the material may appear overly "stiff" in simulations, potentially leading to an overestimation of its dynamic load-bearing capacity and a tendency toward brittle failure. Conversely, if C is set too low, the material may behave unrealistically "soft", underestimating its dynamic strength and exhibiting more ductile failure characteristics.

The damage function, the pressure for fully dense material and its volumetric strain are shown in

$$D = \sum \frac{\Delta \epsilon_{\rm p} + \Delta \mu_{\rm p}}{D_1 \left(p^* + T^* \right) D_2} \tag{7}$$

$$p = K_1 \bar{\mu} + K_2 \bar{\mu}^2 + K_3 \bar{\mu}^3 \tag{8}$$

$$\bar{\mu} = \frac{\mu - \mu_{\text{lock}}}{1 + \mu_{\text{lock}}} \tag{9}$$

where $\Delta \epsilon_{\rm p}$ and $\Delta \mu_{\rm p}$ represent the equivalent plastic strain and the plastic volumetric strain, and D_1 , D_2 , K_1 , K_2 , and K_3 the material constants. $T^* = T/f_{\rm c}'$ is the normalized maximum tensile hydrostatic pressure and $\mu_{\rm lock}$ the locking volumetric strain.

1. 3 Mesoscale model under biaxial loading

Fig.3 depicts a schematic diagram of the biaxial loading for CAC. σ_1 and σ_2 represent the vertical stress on the top (bottom) surface and the horizontal stress on the lateral surface of the specimen, respectively. Generally, σ is taken as positive when the stress is tensile and negative when it is compressive. According to Ref.[11], the biaxial compressive.

sive strength of concrete is greater than its uniaxial compressive strength and this enhancement effect depends on the ratio of horizontal stress to vertical stress (σ_2/σ_1), commonly defined as the stress ratio α . Following the biaxial test method employed by $\mathrm{Li}^{[6]}$, this study uses displacement-controlled loading for biaxial simulations.

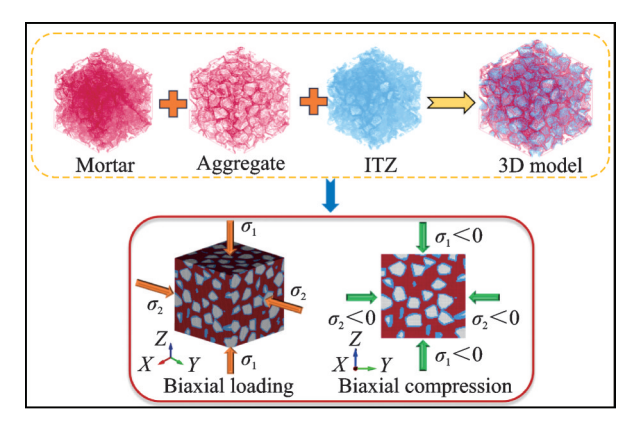


Fig.3 Schematic diagram of biaxial loading

1.4 Validation of mesoscale model

Li^[6] studied the biaxial compressive mechanical properties of CAC under different stress ratios $(\alpha = 0.25, 0.5, 0.75, \text{ and } 1)$. A numerical analysis of the biaxial compressive mechanical behavior of C40 CAC with a stress ratio $\alpha = 0.75$ is conducted based on the aforementioned mesoscale model and material parameters. Furthermore, since Li's [6] experimental results do not take systematic errors into account, we correct these errors. A comparison between the corrected experimental and the numerical results is presented. The failure modes and stress-strain curves are shown in Fig.4. As can be seen in Fig.4(a), the CAC specimens exhibit diagonal shear failure characteristics under biaxial stress conditions. As the load increases, two diagonal cracks appear at the bottom edge. Under the combined action of vertical and lateral pressures, these two cracks propagate diagonally and eventually converge near the central point of the top surface. The experimental results of the biaxial failure mode are consistent with the numerical results, indicating that the mesoscale model can be used to simulate the biaxial compressive failure characteristics of CAC. Fig. 4(b) compares the experimental and numerical

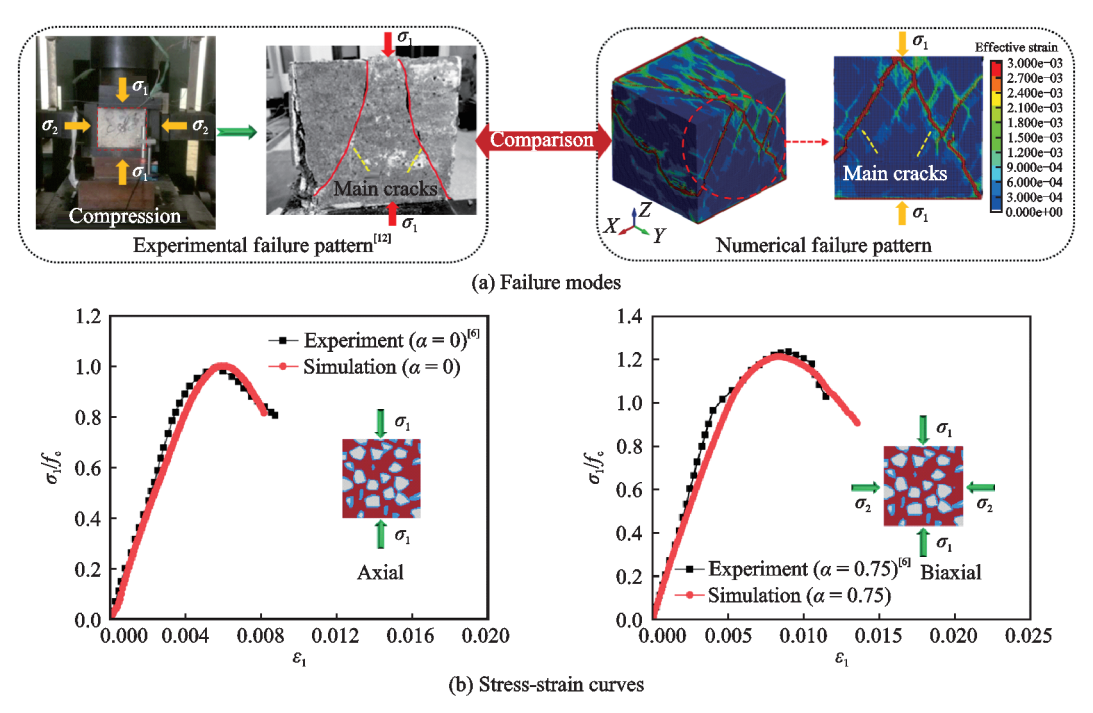


Fig.4 Comparison of experimental and numerical results of CAC

stress-strain curves of C40 CAC under uniaxial compression ($\alpha = 0.75$). As shown in Fig.4(b), both the uniaxial and biaxial results from the numerical analysis align well with experimental results of Ref.[6]. This agreement includes the ascending and descending portions of the curves, as well as the peak stress values.

In summary, this mesoscopic simulation method demonstrates high reliability and accuracy in analyzing the biaxial mechanical properties and failure modes of CAC. Therefore, this mesoscale model and the corresponding material parameters will continue to be used to study the biaxial mechanical behavior of C40 CAC under different stress ratios ($\alpha=0,0.1,0.25,0.5,0.75,$ and 1). This will encompass the failure modes, failure processes, and stress-strain relationships of the specimens. Ultimately, based on the numerical results, appropriate biaxial failure criteria and strength envelopes will be established.

2 Mechanical Behaviors of CAC Under Biaxial Stresses

2. 1 Failure mode

Fig.5 shows the failure modes of CAC under

biaxial compressive loading. As can be seen from the figure, the failure modes of CAC under biaxial stresses differ from those under uniaxial stress. Under biaxial compressive loading, CAC primarily exhibits diagonal shear failure. Li's [6] experimental results indicate that diagonal cracks appear on the surface perpendicular to the lateral pressure. These diagonal cracks gradually expand into diagonal fracture planes along the direction of the lateral pressure. The specimens exhibit characteristics of diagonal shear failure, which is highly consistent with the numerical results presented in this paper. Guo's[13] research indicates that the failure mode of OPC under biaxial compression typically manifests as columnar crushing or lamellar splitting. Diagonal shear failure usually occurs under triaxial stress conditions. However, such failure mode is observed in the biaxial loading of CAC. The possible reason is that the performance of CAC is similar to that of lightweight aggregate concrete (LAC), exhibiting higher brittleness compared with OPC and highstrength concrete (HSC), which is determined by the characteristics of coral aggregate. Coral aggregate has low strength and is porous. After macro cracks form in the specimen, the pores within the aggregates are compacted. The cracks rapidly propagate into the cement paste, leading to more severe damage. Based on the experimental and numerical results, it can be observed that when the specimen is subjected to both vertical and lateral loads, numerous micro-cracks develop inside and on the surface of the specimen, resulting in failure modes different from that under uniaxial loading. Additionally, it can be seen that the failure modes are also related to the stress ratio. As the stress ratio increases from 0.1 to 1, the angle between the main crack and the vertical loading surface gradually decreases.

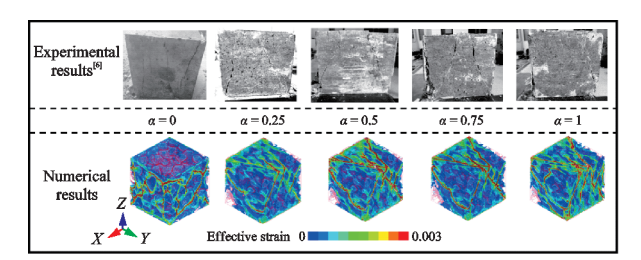


Fig.5 Failure modes of CAC under biaxial compression

Fig.6 illustrates the failure process of CAC under biaxial compressive loading with a stress ratio of 0.75. As the loading progresses, the specimen initially develops some micro-cracks. Subsequently, internal micro-cracks increase gradually and propagate to form interconnected cracks, leading to plastic deformation. With further increase in load, the cracks continue to propagate, eventually resulting in two diagonal main cracks appearing at the bottom edge. The width of the cracks also increases continuously. These two diagonal cracks extend and converge near the center point on the top surface of the specimen, ultimately causing concrete failure at the limit strain. In summary, the numerical results exhibit a high degree of agreement with Li's [6] experimental results, indicating that the mesoscale model can effectively simulate the mechanical behavior and failure process of CAC under biaxial stress conditions.

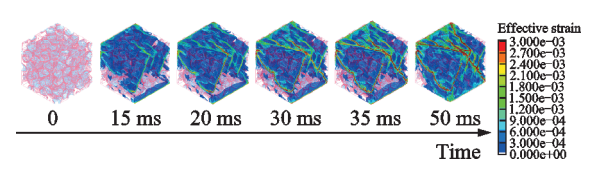


Fig.6 Typical failure process of CAC under biaxial compression ($\alpha = 0.75$)

During the simulation process, it is observed that the failure cracks in CAC penetrate through the coral aggregates, as depicted in Fig. 7. This is consistent with conclusions drawn by Da et al.[3], Zhou et al.[14], and Fu et al.[15]. Normal aggregates in OPC typically have higher strength and the weak zones are mainly concentrated at the ITZ, where cracks tend to propagate, as shown in Fig.8(a). Coral aggregates exhibit lower strength, and the rough surfaces enhance the bond strength at the interface between the aggregate and mortar. Additionally, the porous characteristics of coral aggregates allow cement paste to penetrate the small pores, enhancing the mechanical interlock with the aggregate and thereby strengthening the ITZ. The ITZ in CAC demonstrates stronger performance compared with OPC. Therefore, the aggregates replace the ITZ as the weak zone in CAC. During the compression process, cracks penetrate through the coral aggregates. The failure of the aggregates accelerates the damage to the cement mortar, resulting in a failure mode characterized by the splitting of the aggregates, as depicted in Fig.8(b).

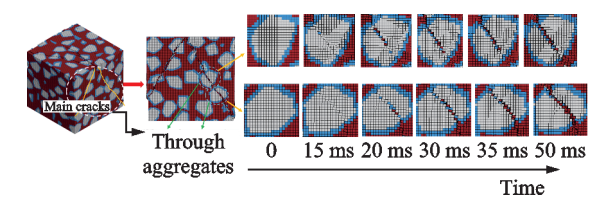


Fig.7 Failure process of coral aggregates

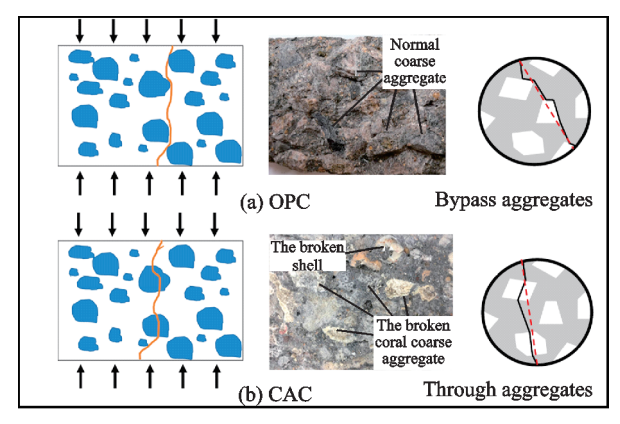


Fig.8 Failure mechanism diagrams of CAC and OPC

2. 2 Stress-strain curve

Fig.9 shows the stress-strain curves of CAC under biaxial compressive loading with stress ratios

of 0, 0.1, 0.25, 0.5, 0.75, and 1. It is evident from the figure that the stress-strain curves of CAC exhibit similar development trends under different stress ratios. The stress ratio of 0 represents the uniaxial compression condition. Comparing the stress-strain curves of CAC under uniaxial and biaxial compressive loading, it can be observed that the initial slope of the rising segment and the peak stress under biaxial loading are greater than those under uniaxial loading. This indicates that the elastic modulus and compressive strength of C40 CAC are higher under biaxial loading. The main reason is that the lateral loads effectively restrain the expansion of cracks in concrete, enhancing its linear elastic behavior and compressive strength. This finding is consistent with conclusions from Refs.[11,16]. Furthermore, CAC exhibits a clear intermediate principal stress effect. The ultimate strength in the direction of the maximum principal stress initially increases and then decreases with increasing stress ratio. This trend is similar to the strength behavior observed in OPC and high-strength high-performance concrete (HSH- $PC)^{[11,17-19]}$

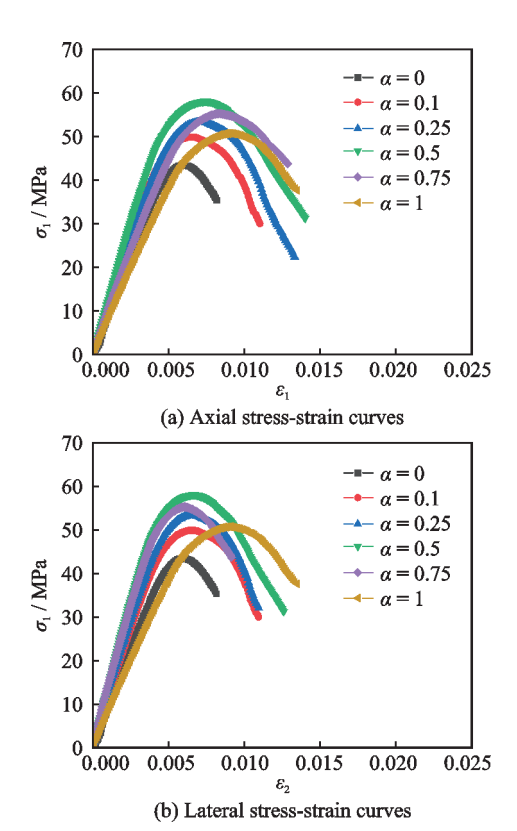


Fig.9 Axial and lateral stress-strain curves of CAC under biaxial compression

Fig. 10 shows the relationship between the biaxial compressive strength and stress ratio of CAC. It shows that as the stress ratio increases from 0.1 to 0.5, σ_1 gradually increases. However, as the stress ratio increases from 0.5 to 1, σ_1 gradually decreases. The biaxial compressive strengths of CAC at stress ratios of 0.1, 0.25, 0.5, 0.75, and 1 are increased by 14.99%, 19.98%, 27.66%, 20.48%, and 13.36% compared with the uniaxial strength, respectively. At a stress ratio of 0.5, CAC exhibits its highest compressive strength, which aligns with Refs. [12, 20-21]. Additionally, Fig. 10 shows that the results for C40 CAC are positioned within those of C30 CAC, indicating that lower-strength CAC experiences a greater increase in main compressive strength under lateral pressure constraint. Conversely, higher-strength CAC shows a smaller increase, suggesting that lower-strength CAC is more sensitive to lateral pressure.

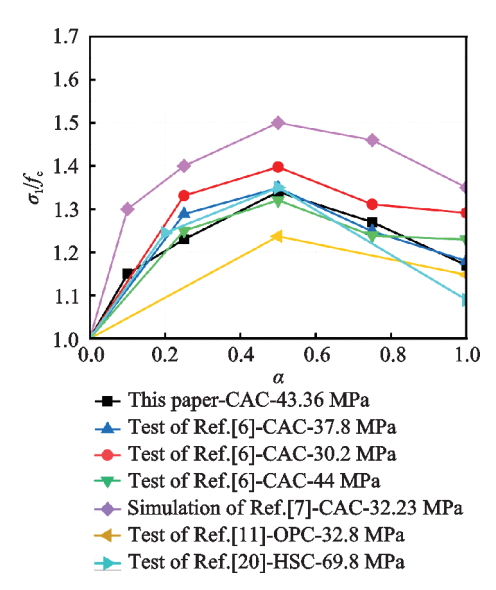


Fig.10 Relationship between biaxial compressive strength and stress ratio of CAC

2. 3 Effect of aggregate volume fraction

Mesoscale models with different aggregate volume fractions are established, with corresponding values of 19.24%, 27.22%, and 37.37%, as shown in Fig.11. Biaxial loading is applied to the models with a controlled stress ratio of 0.5. The biaxial compressive stress-strain curves for different volume fractions are presented in Fig.12. The re-

sults indicate that the biaxial compressive strength gradually decreases with increasing aggregate volume fraction. This may be attributed to the fact that coral aggregates, as the weak phase in CAC, tend to undergo crushing failure at an early stage of loading, leading to the overall failure of the specimen. An increase in aggregate volume fraction results in a greater proportion of weak zones within the specimen, making it more susceptible to failure and reducing its compressive strength. A previous study by Wu et al. [22] on the uniaxial compression behavior of CAC with different aggregate volume fractions also showed that the uniaxial compressive strength decreased progressively as the volume fraction increased from 0 to 58.0%. Further research is needed to investigate the effects of even higher aggregate volume fractions.

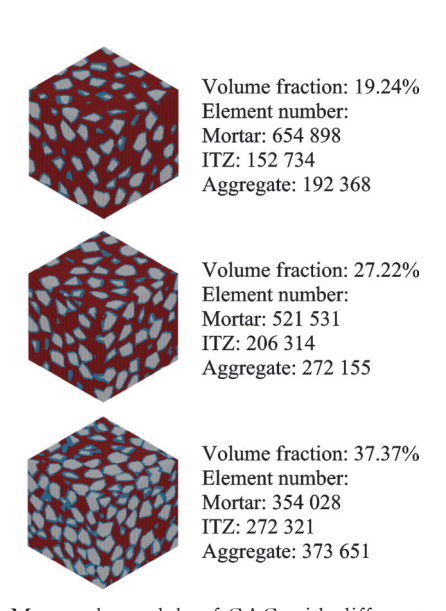


Fig.11 Mesoscale models of CAC with different aggregate volume fractions

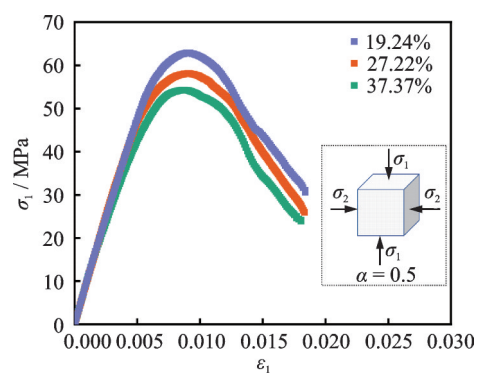


Fig.12 Biaxial compressive stress-strain curves of CAC with different aggregate volume fractions

3 Biaxial Strength and Failure Criteria

The failure criterion (strength criterion) expresses the failure envelope of concrete in the form of mathematical functions. It is the basis for determining whether concrete has reached a state of failure or ultimate strength. Studying the variations in concrete strength and failure criteria under multiaxial stress states is crucial for the rational design and safe operation of structures. Table 2 presents the biaxial compressive strength values of CAC. The most commonly used biaxial failure criterion for concrete was proposed^[11]. The expression for biaxial compression is as follows

$$\left(\frac{\sigma_1}{f_c} + \frac{\sigma_2}{f_c}\right)^2 + \frac{\sigma_1}{f_c} + 3.65 \frac{\sigma_2}{f_c} = 0 \tag{10}$$

where f_c represents the uniaxial compressive strength.

Table 2 Stress values of CAC under biaxial compression

α	σ_1/MPa	$\sigma_{\scriptscriptstyle 2}/{ m MPa}$	$\sigma_{ m 1}/f_{ m c}$	$\sigma_{\scriptscriptstyle 2}/f_{\scriptscriptstyle m c}$
0	-43.36	0	1.00	0.00
0.1	-49.86	-4.99	1.15	0.12
0.25	-53.32	-13.33	1.23	0.31
0.5	-58.11	-29.06	1.34	0.67
0.75	-55.26	-41.15	1.27	0.95
1	-50.74	-50.74	1.17	1.17

Comparing Kupfer's[11] strength criterion with the data from this study, it is found that it does not fit well with CAC. Based on the characteristics of the biaxial compressive failure envelope, a quadratic curve proposed by Zhou et al.[17] (Eq.(11)) is adopted to describe the biaxial compressive strength criterion for CAC, where A, B, C, and D are parameters. Fitting Eq.(11) to the biaxial compressive data points of CAC yields results, as shown in Fig.13(a). It can be observed from Fig.13 that this strength criterion effectively describes the numerical results of this study and the experimental results of Ref.[6], indicating that Zhou's^[17] strength criterion is applicable to CAC. Furthermore, Fig.13(b) compares the failure envelopes of different concretes. It shows that the envelope of

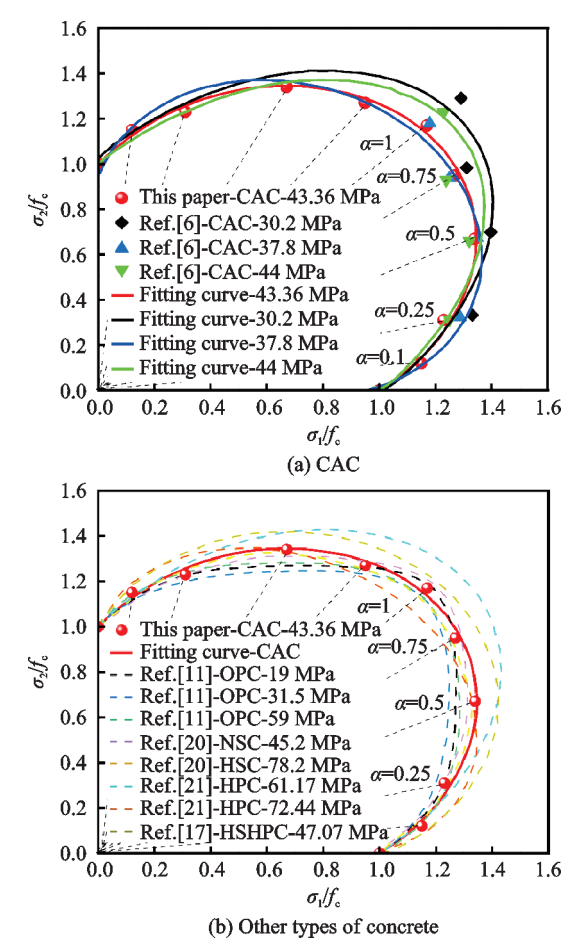


Fig.13 Strength envelopes of CAC and other types of concrete under biaxial compression

CAC is similar to that of normal strength concrete (NSC) proposed by Hussein et al. [20] at the same strength grade. The envelopes proposed by Kupfer et al. [11] and Hussein et al. [20] for OPC and HSC are inside the envelope of CAC, while those proposed by Hample et al. [21] and Zhou et al. [17] for HPC are outside the envelope of CAC.

$$A\left[\left(\frac{\sigma_1}{f_c}\right)^2 + \left(\frac{\sigma_2}{f_c}\right)^2\right] + B\left(\frac{\sigma_1}{f_c}\right)\left(\frac{\sigma_2}{f_c}\right) + C\left(\frac{\sigma_1}{f_c} + \frac{\sigma_2}{f_c}\right) + D = 0$$
(11)

4 Conclusions

This paper is based on a 3D mesoscale model that considers the actual size, shape, and distribution of aggregates. The mechanical properties, failure modes, failure processes, and failure mechanisms of C40 CAC under biaxial compression are systematically investigated. Additionally, the study

compares numerical results with existing experimental results. Different failure criteria for CAC under various biaxial stress states are established. These criteria are used to analyze the strength patterns of CAC and provide valuable references for the analysis of CAC's mechanical performance and its application in structural design. The primary conclusions are drawn as follows:

- (1) The failure modes of CAC under biaxial compressive stress conditions are diagonal shear failure. During the failure process, cracks penetrate the coral aggregates, indicating that the aggregates are the weak area in CAC.
- (2) The stress-strain curve of CAC under biaxial loading is similar to that under uniaxial loading. The biaxial compressive strength and elastic modulus are both greater than those under uniaxial loading and are related to the stress ratio.
- (3) The presence of lateral loads effectively inhibits the propagation of cracks in the concrete, thereby enhancing its linear elastic behavior and compressive strength.
- (4) CAC exhibits a significant intermediate principal stress effect. Under biaxial compressive stress conditions, the ultimate strength in the direction of the maximum principal stress initially increases and then decreases as the stress ratio increases.
- (5) The biaxial compressive strength of CAC reaches its maximum value when the stress ratio is 0.5, which is consistent with the findings of many researchers regarding OPC and HSC.

References

- [1] YU H F, DA B, MA H Y, et al. Durability of concrete structures in tropical atoll environment[J].

 Ocean Engineering, 2017, 135: 1-10.
- [2] ZHOU L L, GUO S C, ZHANG Z H, et al. Mechanical behavior and durability of coral aggregate concrete and bonding performance with fiber-reinforced polymer (FRP) bars: A critical review[J]. Journal of Cleaner Production, 2021, 289: 125652.
- [3] DAB, YUHF, MAHY, et al. Experimental investigation of whole stress-strain curves of coral concrete[J]. Construction and Building Materials, 2016, 122: 81-89.

- [4] MI Renjie, YU Hongfa, MA Haiyan, et al. Study on the mechanical property of coral concrete[J]. The Ocean Engineering, 2016, 34(4): 47-54. (in Chinese)
- [5] SU Chen, MA Haiyan, YU Hongfa, et al. Effect of different coral aggregates on mechanical properties of coral concrete[J]. Journal of the Chinese Ceramic Society, 2020, 48(11): 1771-1780. (in Chinese)
- [6] LI Da. Experimental study of coral sand concrete under uniaxial and biaxial compression[D]. Wuhan: Wuhan University of Technology, 2018. (in Chinese)
- [7] WUZY, YUHF, ZHANGJH, et al. Mesoscopic study of the mechanical properties of coral aggregate concrete under complex loads[J]. Composite Structures, 2023, 308: 116712.
- [8] HOLMQUIST T, JOHNSON G R. A computational constitutive model for glass subjected to large strains, high strain rates and high pressures[J]. Journal of Applied Mechanics, 2018, 78: 051003.
- [9] MALVAR L J, CRAWFORD J E, WESEVICH J W, et al. A plasticity concrete material model for DY-NA3D[J]. International Journal of Impact Engineering, 1997, 19(9/10): 847-873.
- [10] BARNES B D, DIAMOND S, DOLCH W L. Micromorphology of the interfacial zone around aggregates in Portland cement mortar[J]. Journal of the American Ceramic Society, 1979, 62(1/2): 21-24.
- [11] KUPFER H, HILSDORF H K, RUSCH H. Behavior of concrete under biaxial stresses[J]. ACI Journal Proceedings, 1969, 66(8): 656-666.
- [12] REN X D, YANG W Z, ZHOU Y, et al. Behavior of high-performance concrete under uniaxial and biaxial loading[J]. ACI Materials Journal, 2008, 105(6): 548-558.
- [13] GUO Z H. Strength and constitutive relationship of concrete[M]. Beijing: Tsinghua University Press, 1997. (in Chinese)
- [14] ZHOU W, FENG P, LIN H W. Constitutive relations of coral aggregate concrete under uniaxial and triaxial compression[J]. Construction and Building Materials, 2020, 251: 118957.
- [15] FU Q, BU M X, SU L, et al. Dynamic triaxial compressive response and failure mechanism of basalt fibre-reinforced coral concrete[J]. International Journal of Impact Engineering, 2021, 156: 103930.
- [16] ZHANG Y H, CHEN Q Q, WANG Z Y, et al. 3D mesoscale fracture analysis of concrete under complex loading[J]. Engineering Fracture Mechanics, 2019,

- 220: 106646.
- [17] ZHOU J J, PAN J L, ZHANG L, et al. Experimental study on mechanical behavior of high-strength high-performance concrete under biaxial loading[J]. Construction and Building Materials, 2020, 258: 119681.
- [18] LIU T C Y, NILSON A H, SLATE F O. Stress-strain response and fracture of concrete in uniaxial and biaxial compression[J]. ACI Journal Proceedings, 1972, 69(5): 291-295.
- [19] TASUJI M E, SLATE F O, NILSON A H. Stress-strain response and fracture of concrete in biaxial loading[J]. ACI Journal Proceedings, 1978, 75(7): 306-312.
- [20] HUSSEIN A, MARZOUK H. Behavior of highstrength concrete under biaxial stresses[J]. ACI Materials Journal, 2000, 97(1): 27-36.
- [21] HAMPEL T, SPECK K, SCHEERER S, et al. High-performance concrete under biaxial and triaxial loads[J]. Journal of Engineering Mechanics, 2009, 135(11): 1274-1280.
- [22] WUZY, ZHANGJH, YUHF, et al. 3D mesoscopic analysis on the compressive behavior of coral aggregate concrete accounting for coarse aggregate volume and maximum aggregate size[J]. Composite Structures, 2021, 273: 114271.

Acknowledgements This work was supported by the National Science Foundations of China (Nos.52078250, 51878350, 11832013, 51678304, 51508272).

Authors

The first author Mr. CHEN Xusheng received his M.S. degree in Department of Civil and Airport Engineering from Nanjing University of Aeronautics and Astronautics, Nanjing, China. His research interest is multiaxial numerical simulation of concrete.

The corresponding authors Dr. MA Haiyan received his Ph.D. degree in School of Civil Engineering from Southeast University. She is currently a associate professor in College of Intelligent Construction of Jishou University. Her research interests include mechanical properties and numerical simulation of concrete. Prof. YU Hongfa received his Ph.D. degree in School of Materials Science and Engineering from Southeast University. He is currently a professor and doctoral supervisor in College of Civil Aviation of Nanjing University of Aeronautics and Astronautics. His research interests include durability and mechanical properties of concrete.

Author contributions Mr. CHEN Xusheng designed the

study, conducted the simulation and analysis, interpreted the results and wrote the manuscript. Prof. YU Hongfa contributed to data and model components for the CAC model. Dr. MA Haiyan complied the models and checked

the manuscript. All authors commented on the manuscript draft and approved the submission.

Competing interests The authors declare no competing interests.

(Production Editor: XU Chengting)

CAC双轴压缩力学性能的三维细观研究

陈旭升1,麻海燕1,2,余红发1

(1.南京航空航天大学民航学院,南京 211106,中国; 2.吉首大学智能建造学院,张家界 427000,中国)

摘要:关于珊瑚混凝土(Coral aggregate concrete, CAC)的研究主要集中于单轴应力状态。然而,在实际工程中混凝土结构经常处于复杂应力状态。研究多轴应力状态下CAC的力学行为和破坏机理是十分必要的。本文采用一种考虑实际骨料大小、形状和空间分布的三维随机细观模型,通过与已有试验数据的对比,验证了模型和材料参数的可靠性。随后,利用该模型系统研究了C40CAC在双轴压缩工况下的力学性能、破坏模式和破坏过程等,并与已有的CAC和普通硅酸盐混凝土(Ordinary portland concrete, OPC)的试验结果进行对比。结果表明:双轴压缩作用下CAC的破坏模式为斜剪破坏,CAC的双轴抗压强度和弹性模量大于单轴应力状态并表现出显著的中间主应力效应。当应力比为0.5时,双轴抗压强度达到最大值,这与OPC的结论一致。最后,建立了双轴压缩下CAC的破坏准则和强度包络线,为分析CAC的强度特征和结构设计提供参考。

关键词:珊瑚混凝土:双轴压缩:应力比:破坏模式:强度包络线